

Chapter

Tunable Multifunctionality in Heusler Alloys by Extreme Conditions

Devarajan Uthiran and Arumugam Sonachalam

Abstract

The multifunctional materials have demonstrated various properties such as shape memory effect (SME), magneto caloric effect (MCE), magneto resistance (MR), piezoresistance (PR), exchange bias (EB), half metallic ferromagnetism (HMF), and spin polarization. Among many Heusler compounds, Ni-Mn-Ga alloys provide SME, MCE, PR, and MR behaviors. These properties can be tuned by some external/internal perturbations such as pressure, magnetic field, and chemical composition. These alloys are prepared using an arc melting furnace under by melting the high-purity starting elements (99.99%). The aim of the book chapter is to enhance the multicaloric properties (MCE and PR) nearer to ambient temperature by the application of some external parameters. Hence, we have chosen few Heusler alloys. These materials are investigated under extreme conditions (hydrostatic pressure, high magnetic field, and low temperature). All the doped and undoped Ni-Mn-Ga alloy series alloys exhibit conventional MCE. The application of external magnetic field increases the magnetization for both alloys. The hydrostatic pressure influences M_s and broadens the hysteresis width in both the samples. The observed metamagnetic transition at ambient pressure gets suppressed at higher pressure. Also, high pressure induces larger magneto crystalline anisotropy. The effect of pressure on MCE is decreased for both $Ni_{2-x}Mn_{1+x}Ga$ ($x = 0$ and 0.15) alloys. These alloys exhibit -ve PR ($x=0 @ 30$ kbar) and +ve PR ($x = 0.15 @ 28$ kbar) when subjected to hydrostatic pressure. The rate of change of T and resistivity with respect to pressure are calculated and show positive values for both the samples. The residual resistivity and electron-electron scattering factor are found to be decreased with pressure for $x = 0$, and it exhibits metallic behavior. However, both parameters increase for $x = 0.15$ alloy, and it may be related to static disorder effects and spin fluctuations.

Keywords: Heusler alloys, NiMnGa, magneto caloric effect, magnetoresistance, piezoresistance

1. Introduction

1.1 Investigation of the influence of hydrostatic pressure on the magnetic magnetocaloric properties, electronic transport, and piezoresistivity of $\text{Ni}_{2-x}\text{Mn}_{1+x}\text{Ga}$ ($x = 0, 0.15$) Heusler alloys

The discovery of new phase transformations can be performed through high-pressure studies. The hydrostatic pressure effect gives insistently to recognize the physical stuff of ingredients adjacent to the phase transitions with correlating phenomenon. Within various stages happening in scheme of magnetic shape memory, they exhibit phases at high and low temperature, high (austenite) and low (austenite). The self-generated lattice strain is brought by martensite transformation in Heusler alloys at low temperature. Freshly, the series of Ni-Mn alloys have been fascinating for numerous uses because of the concerning multifunctional assets such as shape memory effect (SME) [1, 2], magneto caloric effect (MCE) [3, 4], exchange bias (EB) behavior [5], and magneto resistance (MR) [6–10]. In the foresaid credible tenders, the resources having MCE demonstrations predict for custom in condensed matter cooling system. Within the diverse magnetic shape memory alloys, Ni-Mn-Ga has premeditated widely; afterward, enormous strain was developed by magnetic field. The samples endure first-order structural alteration from extraordinary thermal austenite to low thermal martensite and consume prominent magnetocrystalline anisotropy in the lower martensite in addition to low twinning stress, which provides magnetic field-induced strain. The change in composition considerably impacts the phase transformations, crystallographic structures, and magnetic properties in NiMnGa alloys [11–16].

Hydrostatic pressures are known to play a significant role on the magnetic and structural properties of these systems [17–19]. The relative stability of the high-temperature cubic phase and the low-temperature martensite phase can be influenced by pressure. Magnetism in these alloys mainly arises from RKKY exchange interaction, within the Mn atoms [20]. The exchange interaction between Mn-Mn atoms in Heusler alloys powerfully influences on the distance and is reformed by either chemical substitutions (or) hydrostatic pressure. These consequences suggest the observation of positive pressure coefficient of $J_{\text{Mn-Mn}}$ [21]. Recently, the effect of pressure on some of the NiMn-based systems has been reported [22–26]. Hydrostatic pressure effect on magnetic and martensitic transition shifts toward higher temperature with decrease of ΔS_{M} in NiMnIn magnetic superelastic alloys [22]. Albertini *et al* reported the pressure effects on MCE in Mn-rich and Ni-rich Ni_2MnGa alloy and found that the MCE decreases (increases) for Ni (Mn)-rich alloy [23]. Kamarad *et al* [27] have studied the effect of hydrostatic pressure on magnetization of Ni-rich $\text{Ni}_{2+x}\text{Mn}_{1-x}\text{Ga}$ ($x = 0, 0.15$) compounds and reported that pressure decreases $\Delta S_{\text{M}}^{\text{max}}$ at T_{M} . Further, Esakki Muthu *et al* [26] have reported the effect of hydrostatic pressure on M_{s} and ΔS_{M} in $\text{Ni}_{50-x}\text{Mn}_{37+x}\text{Sn}_{13}$ ($x = 2, 3$) alloys. Nayak *et al* [24] reported on NiCoMnSb alloy that the pressure enhances the stability of the martensite phase and decreases $\Delta S_{\text{M}}^{\text{max}}$ besides an upward shift in T_{M} . By the hydrostatic pressure effect on the magnetic and magneto caloric property of the Heusler alloys. At the same time, up to now few reports are available on the pressure need of MCE in Mn fertile Ni-Mn-Ga alloys [23].

Band ferromagnetism is a significant phenomenon developed in several transition-metal compounds. High-pressure studies can provide valuable information on electronic structure and electron-electron interactions in intermetallics. Among many of

these studies, hydrostatic pressure [24] has been recognized as an effective tool to change physical and chemical properties in solids. Nevertheless, resistivity, piezoresistance (PR) [25], and pressure-induced phase transition [26, 27] are renowned as important phenomena that occur in Heusler alloys. PR is the change in resistance provoked by pressure effect was first discovered by Smith [28] in semiconductors (Si, Ge) possessing anisotropic energy with wide band structures. Further, they are being broadly used as stress and strain sensors [29]. Numerous kinds of Heusler alloy systems such as Ni-Mn-X (X = Sn, Ga, Si, Sb) have been extensively studied [9, 30–48]. Among them, Ni₂MnGa, a potentially well-known magnetic shape memory alloy (MSMA) [1, 31, 32], has been considerably investigated material for both scientific and technological purposes and is known to exhibit various phenomena such as MCE, EB [32], MR, and magnetic-field-induced strain (MFIS) [33–36]. It undergoes structural transformation from cubic austenite (high temperature, high symmetry phase) to low-temperature martensite phase at $T_M = 202$ K [37] and second-order paramagnetic to FM phase transition at $T_C = 376$ K [27]. Additionally, the increased rate of T_M with pressure is 0.55 K/kbar. On the divergent, for Ni_{1.85}Mn_{1.15}Ga ($T_M = 138$ K), T_M is diluted at the rate of -1.08 K/kbar with fixed hydrostatic pressure and magnetic field [38, 39]. The temperature-reliant electrical resistivity $\rho(T)$, whichever frequently employed to separate metals from insulators, band-gap insulators, Anderson localized insulators, has been studied for Ni-Mn-Ga alloys, for instance, Ni₂MnGa_{1-x}B_x (x = 0.03, 0.05) [40], Ni₂MnGa_{1-x}In_x (x = 0.05–0.15) [41], Ni_{2.16}Mn_{0.84}Ga alloy [42], Ni_{2+x}Mn_{1-x}Ga (x = 0–0.2) [9, 43], and Ni_{49.5}Mn_{25.4}Ga_{25.1}, Ni_{51.1}Mn_{24.9}Ga₂₄ alloys [44]. Furthermore, the time-dependent and field-induced hump in the resistivity was also observed in Ga doped Ni-Mn-Sn alloy [45]. Clear view of magneto structural transition has been investigated in Ni_{2.18}Mn_{0.82}Ga [46]. Temperature dependence of electrical resistivity under various hydrostatic pressures has been studied for Ni_{2.14}Mn_{0.84}Ga_{1.02}, Ni_{2.14}Mn_{0.92}Ga_{0.94}, and Ni₂MnGa single crystals [47]. Large value of piezoresistance and magnetoresistance under uniaxial stress has been observed in Ni₄₅Co₅Mn_{37.5}In_{12.5} [48]. In this work, we investigate the effect of hydrostatic pressure on the resistivity and piezoresistivity (PR) of Ni_{2-x}Mn_{1+x}Ga (x = 0, 0.15) magnetic shape memory alloys. We have also determined the ρ_0 and (A) for the alloys.

1.2 Experimental techniques

The samples have been prepared by standard arc melting technique [15, 49]. The elemental ratio is influenced using energy-dispersive analysis of X-rays, which provide the actual chemical ratio as Ni_{1.99}Mn_{1.01}Ga_{1.00} and Ni_{1.9}Mn_{1.15}Ga_{0.95} for x = 0 (Ni₂MnGa) and 0.15 (Ni_{1.85}Mn_{1.15}Ga), respectively. The magnetic studies are accomplished at different pressures by 9 Tesla Physical Property Measurement System (PPMS-9T)-Vibrating Sample Magnetometer (VSM) (Quantum design, USA) module furnished with the Cu-Be clamp-type pressure cell with 10 kbar upper pressure [28]. The thermomagnetic data are recorded with VSM for both cooling and heating mode in the temperature range of 2 K–300 K under ambient and high pressures up to 7.4 kbar for Ni_{1.85}Mn_{1.15}Ga (x = 0.15) and 9.69 kbar for Ni₂MnGa (x = 0) nominal compositions at a constant magnetic field of 0.01 T. The isothermal magnetization M (H) is recorded up to 5 T at ambient and high pressure at different temperatures (180–250 K: x = 0 & 130–160 K: x = 0.15) across T_M . The materials preparation, characterization, and other studies such as isothermal magnetoresistance, magnetization on Ni_{2-x}Mn_{1+x}Ga (x = 0, 0.15) alloys have been discussed [15, 49–51].

High-pressure electrical transport measurements are performed by four-probe resistivity method. Throughout the measurements, the samples with four-probe contacts are immersed in a Teflon capsuled Daphane (#7074) and kept inside the Be-Cu clamp-type hybrid pressure cell (30 kbar). Usual persistent DC current of 80 mA is provided by programmable fixed current source (224, Keithely, USA), voltage is restrained with nanovoltmeter (34420A, Agilent, USA), and temperature is assured through temperature controller (Lakeshore, USA) and is computerized with LABVIEW software. The external pressure is applied to sample using 20 Ton hydraulic press. The clamped pressure cell is externally loaded inside the closed-cycle refrigerator (CCR-VTI). The pressure is standardized using Bi-resistive transitions of Bi I–II (25.5 kbar) and II–III (27 kbar) at ambient as well as least temperature was reached (300– K) employing CCR-VTI. Expanding with turbo molecular pump, the cavities have been vacuumized up to 10^{-6} mbar. A sufficient He gas is entered into container of CCR-VTI when the alloy is cooled, and the temperature of the alloy is suppressed by the compressor. An external mechanical refrigerator removes the warm helium vapor.

2. Results and discussion

The temperature dependence of magnetization M (T) is measured for $\text{Ni}_{2-x}\text{Mn}_{1+x}\text{Ga}$ ($x = 0, 0.15$) alloys at 0.01 and 5 T (**Figure 1**). While cooling from ambient temperature, from $x = 0$, a rapid decrease in magnetization happens at 209 K in the magnetic sources of 0.01 T, which point out the martensitic begins ($M_s = 209$ K). Advanced cooling at less than 188 K (martensite end ($M_f = 188$ K)) results in persistent magnetization up to 5 K. The reduction in magnetization nearby T_M is caused by prominent magneto crystalline anisotropy in the lower-order phase [1, 52]. Here, the T_M is calculated using the relation $T_M = (M_s + A_f)/2$. The hysteresis is noticed between cooling and warming modes, which describes the first-order structural transition. Comparable property is found in the M (T) curve for $x = 0.15$ at a field of 0.01 T (**Figure 1b**), which is in agreement with our earlier M (T) measurement at 0.01 T in $\text{Ni}_{1.84}\text{Mn}_{1.17}\text{Ga}$ in the limited temperature range [50]. The observed M_s values for $x = 0$ and 0.15 are consistent with reported literature [50, 53, 54]. The various characteristic

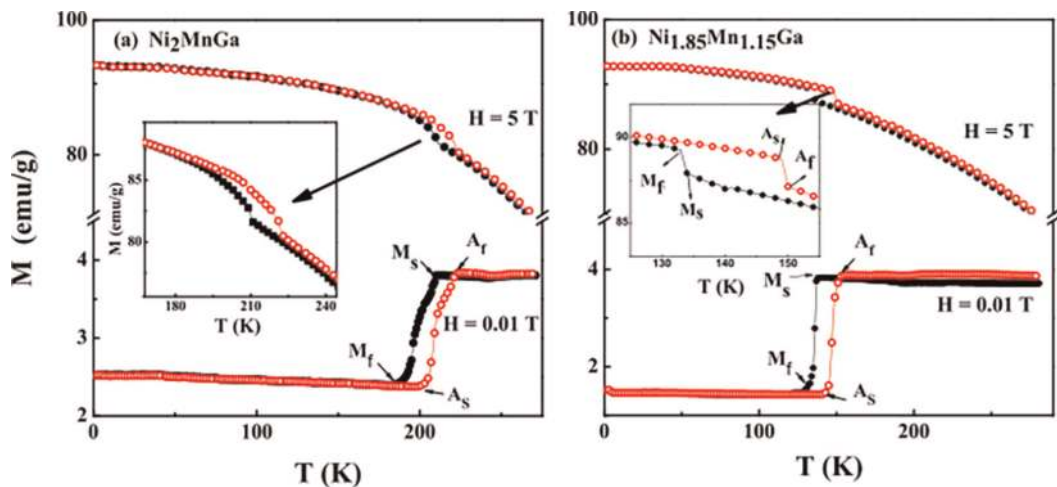


Figure 1. Temperature dependence of magnetization at $H = (0.01 \text{ \& } 5 \text{ T})$ for (a) Ni_2MnGa and (b) $\text{Ni}_{1.85}\text{Mn}_{1.15}\text{Ga}$.

transition temperatures obtained from our M (T) curves are shown in **Tables 1** and **2** for $x = 0, 0.15$. The characteristic transformations decrease with increasing Mn compositions at normal pressure. The closed view of **Figure 1** shows the enlargement of magneto thermal curves information approximate T_M measured. The $H = 5$ T enhances the magnitude of magnetization equated to the lower magnetic field (0.01 T) for both $x = 0$ and 0.15 (**Figure 1**). Besides, the magnetization of the low-stability phase is more than that of high-stability phase at 5 T for both alloys. This is owing to the alignment of magnetic domains in the oriented axis, it destroys the magneto crystalline anisotropy at $H = 5$ T [55, 56]. Similar increase in magnetization with the application of magnetic field has also been observed in $Ni_{1.84}Mn_{1.17}Ga$, $Ni_{50+x}Mn_{25-x}Ga$ ($x = 0, 2, 3, 5$), and $Ni_{1.75}Mn_{1.25}Ga$ [50, 57, 58].

Figure 2 indicates thermo-magnetization with cool and warm modes at different hydrostatic pressures up to 9.69 kbar ($x = 0$) and 7.4 kbar ($x = 0.15$) at $H = 0.01$ T. Notification from **Figure 2a** that M_s increases slightly with pressure, because of hybridization among Ni-3d and Mn/Ga atom. **Table 3** displays pressure-derived function of M_s and T_M equated to existing reports. The hysteresis found in both cool and warm curvatures appears to be extended with enhancement of hydrostatic pressure. The possibility of owing to the variation in magneto crystalline anisotropy at minimum temperature in lower-order phase. Related pressure reliance has been described in $x = 0$ [54], where the heating and cooling curves show opposite trend compared with the present results.

Figure 2b demonstrates the M (T) curve at several hydrostatic pressures (0–7.4 kbar) for $Ni_{2-x}Mn_{1+x}Ga$ ($x = 0.15$). It is originated that M_s and T_M suppress as the pressure enhances ($dM_s/dP = -2.027$ K/kbar); $dT_M/dP = -1.081$ (K/kbar). At the same time, Albertini *et al* [23] noticed that martensitic transformation temperatures raise by pressure for $Ni_{1.9}Mn_{1.3}Ga_{1.8}$. The negative alteration of M_s graces the stability of cubic higher-order phase representing that martensite phase is low stability with

Pressure (kbar)	Transition temperatures (K)				
	M_s	M_f	A_s	A_f	$T_M = (M_s + A_f)/2$
0	209	188	205	222	216
1.37	209	185	208	227	218
6.06	210	209	212	230	220
9.69	210	212	213	233	222

Table 1.
 Transition temperatures with several hydrostatic pressures of Ni_2MnGa .

Pressure (kbar)	Transition temperatures (K)				
	M_s	M_f	A_s	A_f	$T_M = (M_s + A_f)/2$
0	137	128	142	152	144.5
3.0	133	117	141	146	139.5
5.8	128	113	140	147	137.5
7.4	122	101	136	151	136.5

Table 2.
 Transition temperatures with different hydrostatic pressures of $Ni_{1.85}Mn_{1.15}Ga$.

Sample	dT_M/dP (K/kbar)	dM_S/dP (K/kbar)
Ni_2MnGa	0.619	0.103
$Ni_{1.85}Mn_{1.15}Ga$	-1.081	-2.027
$Ni_{2.15}Mn_{0.85}Ga$ [23]	0.58	—
$Ni_{1.9}Mn_{1.3}Ga_{1.8}$ [23]	1.7	—
$Ni_{2.151}Mn_{0.771}Ga$ [59]	0.6	—
$Ni_{48}Mn_{39}Sn_{13}$ [60]	—	3.16
$Ni_{47}Mn_{40}Sn_{13}$ [60]	—	0.51

Table 3.
Pressure derivative values of T_M and M_S for various NiMnGa (Sn) systems.

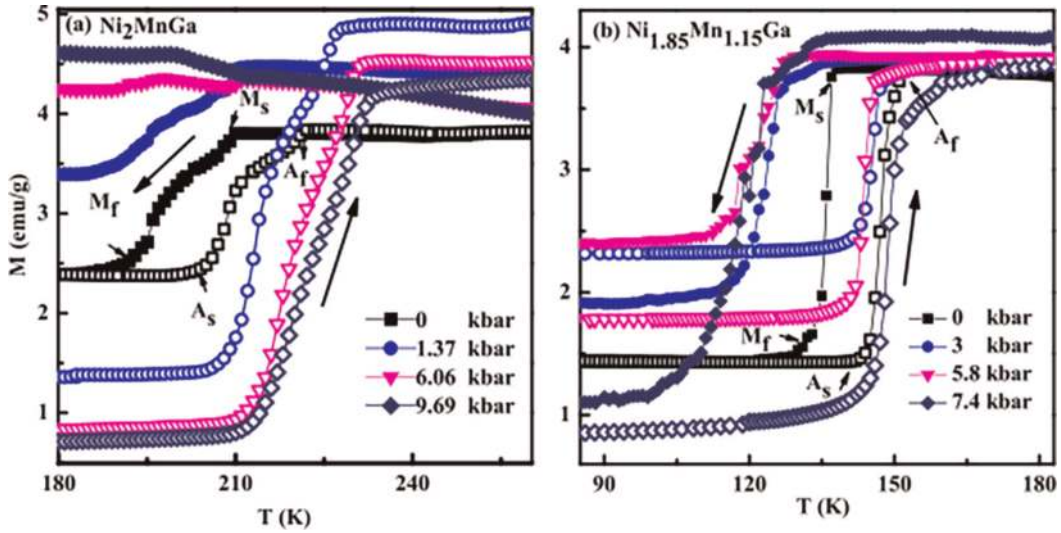


Figure 2.
Thermomagnetic curves (both cool and warm) of $Ni_{2-x}Mn_{1+x}Ga$ ($x = 0, 0.15$) alloys with various applied pressures at $H = 0.01$ T.

pressure. Furthermore, substantial alterations happen in electronic structure under pressure and may extend to various transformation temperatures. Pressure steadies the lower-order phase in further FM shape memory alloys (FSMAs) [61]. In addition, a large width of the hysteresis is noticed on increasing the pressure that is attributed to the enhancement of magneto elastic coupling with lattice strain, twin boundary motion, and first-order transition [61].

Pressure habituation of transformation in $x=0, 0.15$ is represented in **Figure 3**, which confirmed that transformation rises with pressure in $x=0$, while transformation suppresses in $x = 0.15$. This occurrence can be described in following ways. Enhancement of pressure will decrease the crystallographic volume, which affects characteristic transition temperatures. Furthermore, these alloys show that lower volume change with pressure results in slight change in M_S . Kim *et al*, described the pressure reliance of T_M in $x = 0$ and $Ni_{2.14}Mn_{0.84}Ga_{1.02}$ and established high volume change [39]. However, the volume change in our present alloys is lower than the reported $Ni_{50-x}Mn_{37+x}Sn_{13}$ ($x = 2, 3$) [60] and $Ni_{50}Mn_{34}In_{16}$ [22]. The characteristic

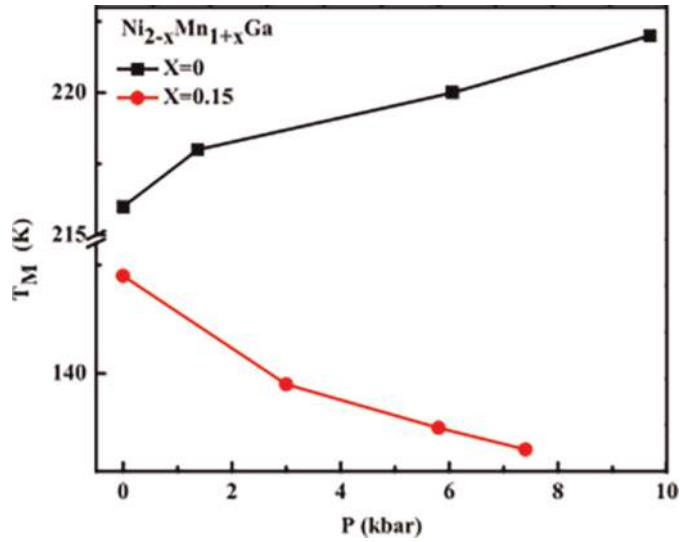


Figure 3. Pressure reliance of T_M in $Ni_{2-x}Mn_{1+x}Ga$ ($x = 0, 0.15$) evaluated at $H = 0.01 T$ under different hydrostatic pressures.

transition temperatures under different pressure are given in **Tables 1** and **2** for both alloys respectively.

The isothermal curves have restrained in $x = 0$ around T_M (180 K–250 K) at ambient, high pressures (**Figure 4a** and **b**). The magnetization work is absorbed into two ways: magnetic field is improved 0–5 and reduced 5–0 T. It is observed that magnetic field prompted first-order metamagnetic transition arises at 220 K, ambient pressure for $x = 0$ (**Figure 4a**). The enclosure of **Figure 4a**) displays the transition clearly. However, this transition disappears at 9.69 kbar. Related actions have been detected in $Ni_{2.208}Mn_{0.737}Ga$ [59]. From **Figure 4b**, the crossover in magnetization is noticed in the $M(H)$ curve approximately 190–235 K. The magnetization is hard to impregnate for temperatures 190 and 196 K specifying a martensite phase, although at austenite phase at 223 K and 235 K the magnetization is relaxed to saturate. This is because of the firm magnetocrystalline anisotropy around transformations in $x = 0$ at high pressure. **Figure 4c** and **d** shows the isothermal curve of $x = 0.15$ at $P = 0, 7.4$ kbar. This $M(H)$ is assessed with rate of temperature 130 K–160 K in gradual rise of 2 K; even though only picked out readings are drawn in **Figure 4c** and **d** for the clear visibility. At normal pressure, the field brought metamagnetic transition is seen in low field (0.68 T) at 146 K insert (**Figure 4c**). But, this transition is blocked at 7.4 kbar (**Figure 4d**). Similar to $x = 0$, the cusp in magnetization has been perceived between martensite and austenite temperature for $x = 0.15$ at $P = 7.4$ kbar, as viewed in (**Figure 4d**). Therefore, the subjection of pressure develops large magnetocrystalline anisotropy in both alloys.

The entropy change in magnetization (ΔS_M) at various pressures is evaluated using the Maxwell's relation

$$\Delta S_M = \int_0^H \left(\frac{\partial M(H, T)}{\partial T} \right)_H dH \quad (1)$$

ΔS_M is computed from the over equation using numerical integration of the isothermal curves. ΔS_M with temperature for various pressures is represented in

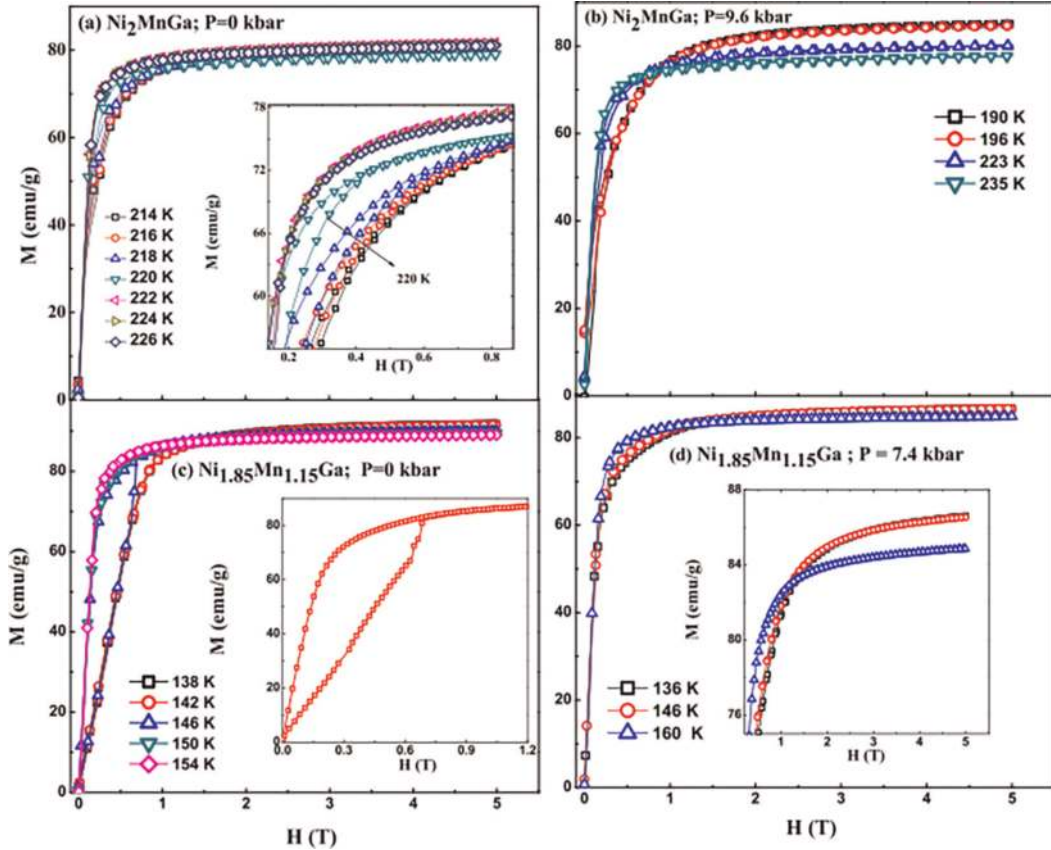


Figure 4. Isothermal curves of $x = 0$ (a) ambient and (b) 9.69 kbar pressure, $x = 0.15$ (c) ambient and (d) 7.4 kbar pressure.

Figure 5. The usage of pressure declines the ΔS_M is $19.21 \text{ Jkg}^{-1}\text{K}^{-1}$ ($P = 0$ kbar) to $6.04 \text{ Jkg}^{-1}\text{K}^{-1}$ ($P = 9.69$ kbar) for $x = 0$. Nevertheless, the peak temperature of ΔS_M gains in the direction of higher temperature with pressure. Enhancement of the maximum temperature of ΔS_M near room temperature with the application of higher pressure. The degree of ΔS_M suppresses from $8.9 \text{ Jkg}^{-1}\text{K}^{-1}$ ($P = 0$) to $1.27 \text{ Jkg}^{-1}\text{K}^{-1}$ ($P = 7.4$ kbar) in $\text{Ni}_{1.85}\text{Mn}_{1.15}\text{Ga}$ and the highest temperature of ΔS_M moves near to lower temperature. Likewise, for Ni-rich $\text{Ni}_{2.208}\text{Mn}_{0.737}\text{Ga}$, ΔS_M shrinkages from $96 \text{ Jkg}^{-1}\text{K}^{-1}$ ($P = 0$) to $86 \text{ Jkg}^{-1}\text{K}^{-1}$ ($P = 8$ kbar) [59]. Additionally, in $\text{Ni}_{2.15}\text{Mn}_{0.85}\text{Ga}$, ΔS_M reduces from $24 \text{ Jkg}^{-1}\text{K}^{-1}$ ($P = 0$) to $20 \text{ Jkg}^{-1}\text{K}^{-1}$ ($P = 11.7$ kbar); however, in Mn-rich $\text{Ni}_{1.9}\text{Mn}_{1.3}\text{Ga}_{0.8}$, ΔS_M promotes from $4.5 \text{ Jkg}^{-1}\text{K}^{-1}$ ($P = 0$) to $6 \text{ Jkg}^{-1}\text{K}^{-1}$ ($P = 12.2$ kbar) [23]. Based on the earlier reports, it is concluded that pressure stimulates additional magnetic entropy in prominent additional Mn in $\text{Ni}_{2-x}\text{Mn}_{1+x}\text{Ga}$ compounds equated to the $x = 0.15$ sample analyzed and excess Ni in $\text{Ni}_{2-x}\text{Mn}_{1+x}\text{Ga}$.

Temperature dependence of resistivity ρ (T) is measured for polycrystalline $\text{Ni}_{2-x}\text{Mn}_{1+x}\text{Ga}$ ($x = 0, 0.15$) at several hydrostatic pressures both in cool and warm sequences. In order to see the clear features, the heating cycle graph has presented for pressure (Figure 6) and the cool-warm lines are prearranged as inside view of Figure 6 at least and maximized pressure. At normal pressure, ρ falls with decrement of temperature in $x = 0$ (Figure 6a) and exhibits least thermal hysteresis near martensite transition. This specifies that structural transitions are specified in the closed view of Figure 6a. Comparable ρ (T) is identified for $x = 0$ [47]. These results are perceived as

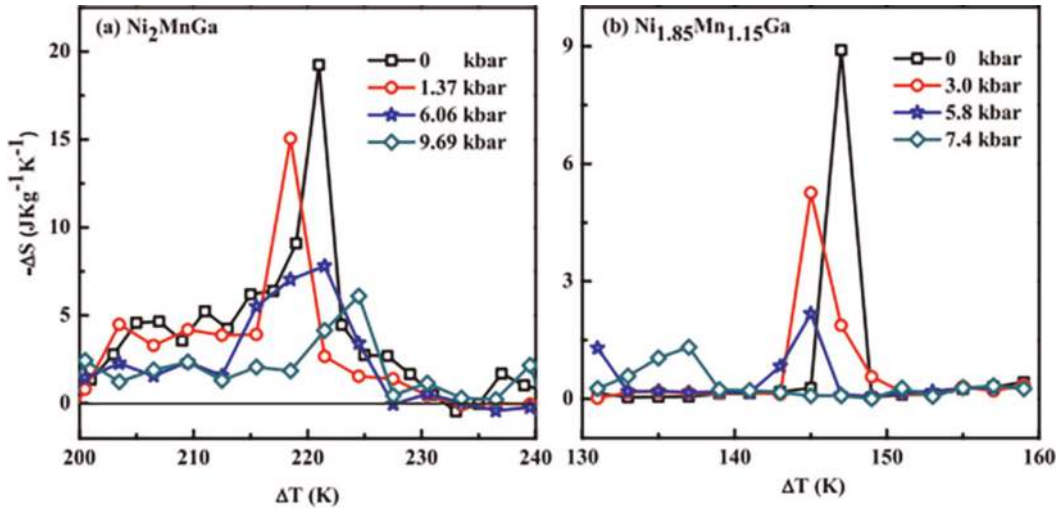


Figure 5. Temperature desirable of magnetic entropy change in $Ni_{2-x}Mn_{1+x}Ga$ ($x = 0, 0.15$) alloys at different hydrostatic pressures.

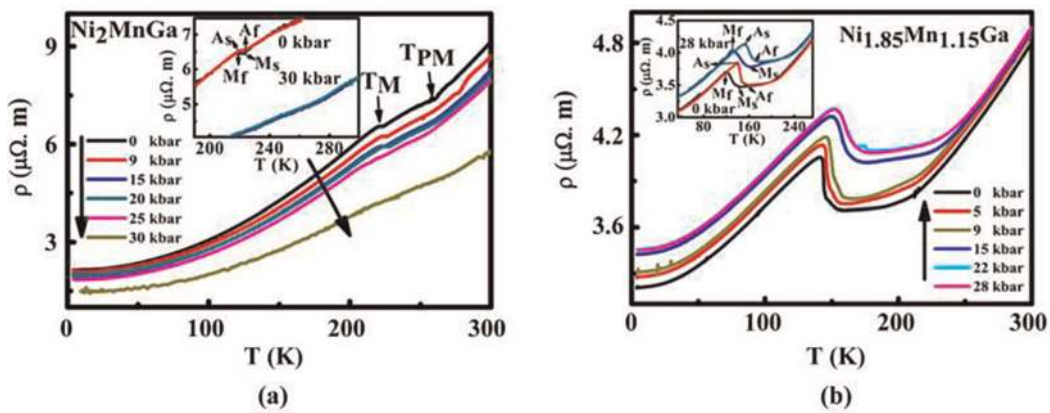


Figure 6. Temperature dependence of resistivity for (a) Ni_2MnGa , (b) $Ni_{1.85}Mn_{1.15}Ga$ alloys at various pressures. Inset: shows ρ vs T in the temperature region of 180–300 K for the pressure of 0 kbar and 30 kbar.

hysteresis curves at ambient and $P = 7$ kbar. The fascinating report at 25 kbar pressure, the hysteresis graph gets repressed in $x = 0$, at 30 kbar, the hysteresis completely be wiped out, and it can be evidently seen in inset of **Figure 6a**. As increasing pressure, its ρ decreases entire 4–300 K and boosts the metallic nature in the alloy due to enriched hybridization of valence band by applied pressure [40, 62, 63]. A mark of the pre-martensite transition (T_{PM}) detected at 260 K at ambient pressure for $x=0$. The cross of the T_{PM} is not clearly witnessed at higher pressure (30 kbar) (**Figure 6a**). The magnetic field and hydrostatic pressure are significantly affected on T_M and T_{PM} of Ni_2MnGa system [39, 64]. Similar $\rho(T)$ has been found for $x = 0.15$ (**Figure 6b**), where the application of pressure increases the ρ due to the pressure-induced phase transformation, which indicates the phase changes from pre-martensite to martensite [46, 47]. Still, total ρ for $x = 0.15$ is lower than $x = 0$. Besides, in demarcation to $x = 0$, considerable thermal hysteresis is seen for entire pressure. This may be related to electronic structure as compared with magnetic actions [19, 63, 65]. The application of pressure shifts the transformation temperature to higher values, and the clear view of transformations for $x = 0.15$ is illustrated from the inset **Figure 6b**.

Figure 7 displays the pressure addition of T_{av}

$$[T_{av} = (A_s + A_f)/2] \quad (2)$$

Martensite to austenite transition for $x = 0$ and 0.15 , which rises with improvement of pressure. The derivative pressures of T_{av} are 0.15 K/kbar and 0.82 K/kbar for $x = 0$ and 0.15 , respectively. This directs the change in volume with pressure for $Ni_{1.85}Mn_{1.15}Ga$ matched to Ni_2MnGa . The additional Mn atoms will fill the Ga and Ni sites consequential in hybridization between Ni and Mn/Ga states in NiMnGa alloy [63]. The application of pressure increases the exchange interactions between Mn-Mn ions, which enhance the hybridization between Ni and Mn/Ga. This needs more thermal energy to drive martensite transition, which in turn increases the characteristic transformation temperature [66, 67]. An important aspect is that width of the hysteresis (given by the difference of $(A_s+A_f)/2$ and $(M_s+M_f)/2$) [68] decreases. This implies larger mobility of the twin boundaries with the application of hydrostatic pressure.

The temperature dependence of piezoresistivity (PR) of $Ni_{2-x}Mn_{1+x}Ga$ ($x = 0, 0.15$) alloys at various pressures is computed using the relation

$$PR(T) = [\rho_P(T) - \rho_A(T)]/\rho_A(T) \quad (3)$$

where ρ_P and ρ_A are resistivity at pressure (P) and ambient pressure. Fascinatingly, PR has negative and positive sign for $x = 0$ and 0.15 (**Figure 8**). The highest PR is found at the martensite transition (near T_M) for all pressures. Inset of **Figure 8a** exposes that for $x = 0$, negative PR gradually enhances with pressure and peak value of $-PR$ is 34% mentioned at 232 K for $P = 30$ kbar. For $x = 0.15$, a prominent peak of PR is remarked at T_M and the application of pressure increases the $+PR$ (inset of **Figure 8b**). The maximum $+PR$ of 17% is noticed at 154 K for $P = 28$ kbar. The observation of negative and positive PR is stimulated by decrement and increment in resistivity (ρ) with pressure for $x = 0$ and $x=0.15$ presented in inset of **Figure 8a** and **b**. Therefore, it affirms that the PR of $x = 0$ responds with pressure. The PR activities are watched in single crystalline $Ni_{45}Co_5Mn_{37.5}In_{12.5}$ under uniaxial stress and attained peak value of PR 122% [48]. Hereafter, the Ni-Mn-Ga compounds are hardly prospective applications in subject of spintronics by revealing changes of PR.

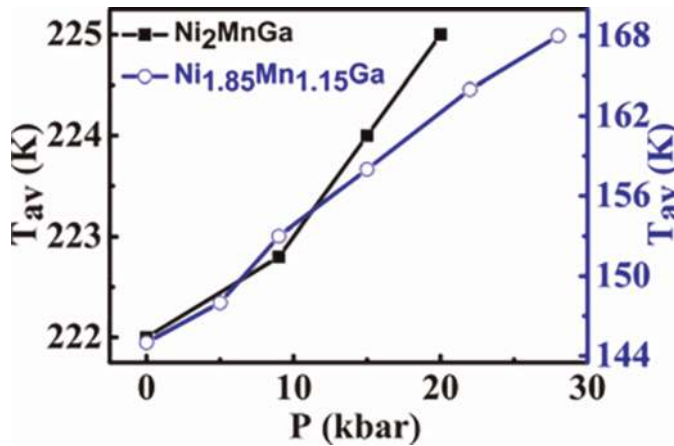


Figure 7. Pressure dependence of T_{av} for $Ni_{2-x}Mn_{1+x}Ga$ ($x = 0, 0.15$) alloys.

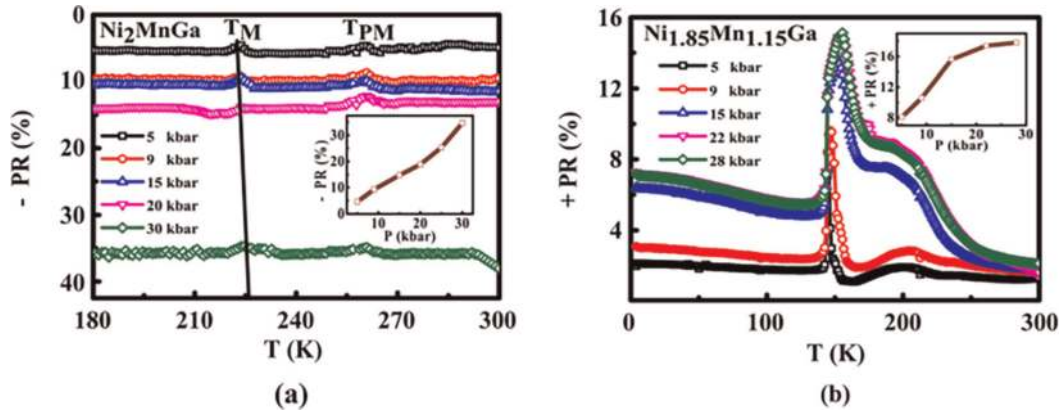


Figure 8. Temperature habituation of PR at various hydrostatic pressures for (a) $x = 0$, (b) $x = 0.15$ alloys. Pressure variant of PR for $x = 0$ and $x = 0.15$ is exposed in insets of a and b.

Figure 9a and b shows variation of both residual resistivity (ρ_0) and electron scattering factor (A) with pressure for $x = 0$ and 0.15. The ρ_0 and (A) are obtained by fitting the simple electrical resistivity equation,

$$\rho = \rho_0 + (AT^2) \quad (4)$$

From the low thermal region 4–200 K ($x = 0$) and 4–130 K ($x = 0.15$) and the curved fitting are displayed in the inset of **Figure 9a and b**. The ρ_0 happens in these alloys due to impurities (or) imperfections. The (A) value at lower thermal region denotes electron-electron scattering [69]. From **Figure 9a**, the rate of ρ_0 and A reductions with pressure for $x = 0$. In demarcation, for $x = 0.15$ mutually ρ_0 and (A) gains with subjected pressure **Figure 9b**. The divergent changes of (A) involve that the subjection of pressure suppresses and enhances the electron-electron scattering for $x = 0$ and $x = 0.15$. In the case of $x = 0.15$, the fixed disorder on because of additional Mn that lodges the Ni locations possibly liable for rises in both the ρ_0 and (A) with pressure [7]. Another factor that might increase (A) could be related to the spin fluctuations due to Fermi surface nesting under pressure [70, 72].

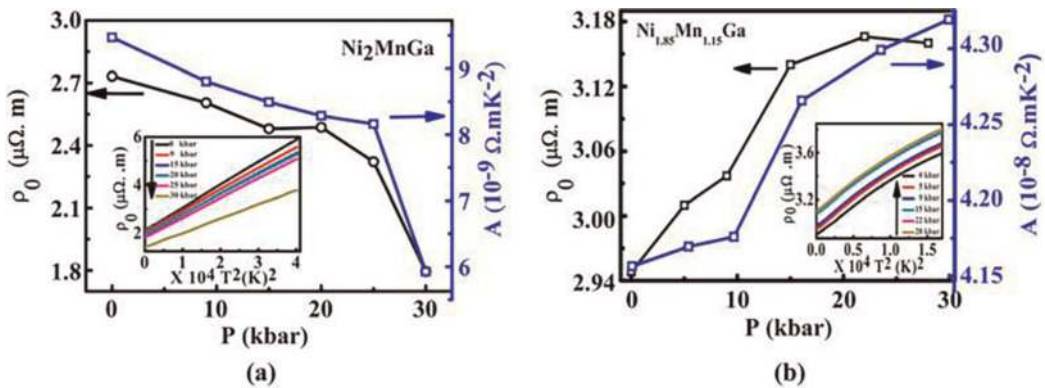


Figure 9. Pressure discrepancy of residual resistivity (ρ_0) and electron scattering factor (A) for (a) Ni_2MnGa (b) $Ni_{1.85}Mn_{1.15}Ga$. The insets of a and b reveals ρ_0 dependence T^2 for Ni_2MnGa and $Ni_{1.85}Mn_{1.15}Ga$.

3. Conclusion

The usage of outward magnetic field raises the magnetization for Ni_2MnGa and $\text{Ni}_{1.85}\text{Mn}_{1.15}\text{Ga}$ alloys. By applying hydrostatic pressure, which includes M_s and expands the hysteresis width in both alloys. The metamagnetic transition is detected at ambient pressure and suppressed at maximum pressure. The high pressure encourages greater magnetocrystalline anisotropy. Finally, the pressure impact on MCE is reduced in ΔS_M for both alloys. In compact of the work, Ni_2MnGa and $\text{Ni}_{1.85}\text{Mn}_{1.15}\text{Ga}$ alloys reveal negative and positive PR, when applied to hydrostatic pressure of 30 kbar and 28 kbar. The rate of variation of T_M and resistivity pertaining to pressure has been computed and exhibits positive numbers for the two alloys. The ρ_0 and (A) are originated to be reduced with pressure for Ni_2MnGa , which exhibit metallic property, merely both rise for $\text{Ni}_{1.85}\text{Mn}_{1.15}\text{Ga}$, and it may be associated to stationary disorder effects and spin oscillations. These materials have incredible potential interest in sensors and spintronics.

Acknowledgements

The author U.D acknowledges DST-SERB-NPDF, UGC-RFSMS-DSKPDF, and S.A and also acknowledges, DST-SERB, BRNS, DRDO, CEFIPRA, DMRL-Hyderabad, and UGC-DAE-CSR-Indore for their financial support and sample preparation, and characterizations.

Conflict of interest

The authors declare no conflict of interest.

Author details

Devarajan Uthiran^{1,2,3*} and Arumugam Sonachalam¹


1 Centre for High Pressure Research, School of Physics, Bharathidasan University, Tiruchirappalli, India

2 Department of Nuclear Physics, University of Madras, Chennai, India

3 Vel Tech Multi Tech Dr. Rangarajan Dr. Sakunthala Engineering College, Chennai, India

*Address all correspondence to: devaraman@gmail.com

IntechOpen

© 2022 The Author(s). Licensee IntechOpen. This chapter is distributed under the terms of the Creative Commons Attribution License (<http://creativecommons.org/licenses/by/3.0>), which permits unrestricted use, distribution, and reproduction in any medium, provided the original work is properly cited. 

References

- [1] Ullakko K, Huang JK, Kantner C, Handley RCO, Kokorin VV. *Applied Physics Letters*. 1996;**69**:1966
- [2] Kainuma R, Imano Y, Ito W, Sutou Y, Morito H, Okamoto S, et al. *Nature (London)*. 2006;**493**:957
- [3] Krenke T, Duman E, Acet M, Wassermann EF, Moya X, Mañosa L, et al. *Nature*. 2005;**4**:450
- [4] Du J, Zheng Q, Ren WJ, Feng WJ, Liu XG, Zhang ZD. *Journal of Physics D: Applied Physics*. 2007;**40**:5523
- [5] Esakki Muthu S, Rama Rao NV, Sridhara Rao DV, Manivel Raja M, Devarajan U, Arumugam S. *Journal of Applied Physics*. 2011;**110**:023904
- [6] Sharma VK, Chattopadhyay MK, Shaeb KHB, Chouhan A, Roy SB. *Applied Physics Letters*. 2006;**89**:222509
- [7] Singh S, Rawat R, Esakki Muthu S, D'Souza SW, Suard E, Senyshyn A, et al. *Physical Review Letters*. 2012;**109**:246601
- [8] Yu SY, Liu ZH, Liu GD, Chen JL, Cao ZX, Wu GH, et al. *Applied Physics Letters*. 2006;**89**:162503
- [9] <https://journals.aps.org/prb/abstract/10.1103/PhysRevB.80.10440444>
- [10] Pathak AK, Gautam BR, Dubenko I, Khan M, Stadler S, Ali N. *Journal of Applied Physics*. 2008;**103**:07F315
- [11] Chernenko VA. *Scripta Materialia*. 1999;**40**:523
- [12] Pons J, Chernenko VA, Santamarta R, Cesari E. *Acta Materialia*. 2000;**48**:3027
- [13] K. Tsuchiya, H. Nakamura, D. Ohtoyo, H. Nakayama, H. Ohtsuka and M. Umemoto, (2001 Interscience Enterprises Ltd, Switzerland, 409.
- [14] Chernenko V, Lvov V, Cesari E, Pons J, Portier R, Zagorodnyuk S. *Materials Transactions, JIM*. 2002;**43**:856
- [15] Banik S, Singh S, Rawat R, Mukhopadhyay PK, Ahuja BL, Awasthi AM, et al. *Journal of Applied Physics*. 2009;**106**:103919
- [16] Banik S, Mukhopadhyay PK, Awasthi AM, Barman SR. *Advanced Materials Research*. 2008;**52**:109
- [17] Kanomata T, Shirakawa K, Kaneko T. *Journal of Magnetism and Magnetic Materials*. 1987;**65**:76
- [18] Kanomata T. *Journal of Magnetism and Magnetic Materials*. 2002;**65**:1987
- [19] Sasioglu E, Sandratskii LM, Bruno P. *Physical Review B*. 2005;**71**:214412
- [20] Kubler J, Williams AR, Sommers CB. *Physical Review B*. 1983;**28**:1751
- [21] Kyuji S, Endo S, Kanomata T, Ono F. *Physica B: Condensed Matter*. 1997;**237**:523
- [22] Mañosa L, Moya X, Planes A, Gutfleisch O, Lyubina J, Barrio M, et al. *Applied Physics Letters*. 2008;**92**:012515
- [23] Albertini F, Kamarád J, Arnold Z, Pareti L, Villa E, Righi L. *Journal of Magnetism and Magnetic Materials*. 2007;**316**:364
- [24] Sagar A, Miller RC. *Journal of Applied Physics*. 1961;**32**:2073

- [25] Bourgault D, Porcar L, Bruyère C, Jacquet P, Courtois P. *The Review of Scientific Instruments*. 2013;**84**:013905
- [26] Chandra Shekar NV, K. Govindarajan, *Bull. Materials Science*. 2001;**24**:1
- [27] Khan M, Dubenko I, Stadler S, Ali N. *Journal of Physics: Condensed Matter*. 2004;**16**:5259
- [28] Smith CS. *Physics Review*. 1954;**94**:1
- [29] Suhling JC, Jaeger RC. *IEEE Sensors Journal*. 2001;**1**:14
- [30] Soderberg O, Ge Y, Sozinov A, Hannula SP, Lindroos VK. *Smart Materials and Structures*. 2005;**14**:S223
- [31] Jakob G, Elmers HJ. *Journal of Magnetism and Magnetic Materials*. 2007;**310**:2779
- [32] Wang B, Liu Y. *Meta*. 2013;**3**:69
- [33] Biswas C, Rawat R, Barman SR. *Applied Physics Letters*. 2005;**86**:202508
- [34] Murray SJ, Marioni M, Allen SM, O'Handley RC, Lograsso TA. *Applied Physics Letters*. 2000;**77**:886
- [35] Liang T, Jiang CB, Xu HB, Liu ZH, Zhang M, Cui YT, et al. *Journal of Magnetism and Magnetic Materials*. 2004;**268**:29
- [36] Sozinov A, Lanska N, Soroka A, Zou W. *Applied Physics Letters*. 2013;**102**:021902
- [37] Webster PJ, Ziebeck KRA, Town SL, Peak MS. *Philosophical Magazine B*. 1984;**49**:295
- [38] Chernenko VA, Lvov VA. *Philosophical Magazine A*. 1996;**73**:999
- [39] Devarajan U, Esakki Muthu S, Arumugam S, Singh S, Barman SR. *Journal of Applied Physics*. 2013;**114**:053906
- [40] Gautam BR, Dubenko I, Pathak AK, Stadler S, Ali N. *Journal of Physics: Condensed Materials*. 2008;**20**:465209
- [41] Kourov NI, Pushin VG, Knyazev YV, Korolev AV. *Physics of the Solid State*. 2007;**49**:1773
- [42] Bozhko AD, Vasilev AN, Khovailo VV, Dikshtein IE, Koledov VV, Seletskii SM, et al. *Journal of Experimental and Theoretical Physics*. 1999;**88**:954
- [43] Vasilev AN, Bozhko AD, Khovailo VV, Dikshtein IE, Shavrov VG, Buchelnikov VD, et al. *Physical Review B*. 1999;**59**:1113
- [44] Chatterjee S, Giri S, De SK, Majumdar S. *Physical Review B*. 2010;**81**:214441
- [45] Khovailo VV, Takagi T, Tani J, Levitin RZ, Cherechukin AA, Matsumoto M, et al. *Physical Review B*. 2002;**65**:092410
- [46] Kim JH, Taniguchi T, Fukuda T, Kakeshita T. *Materials Transactions*. 2005;**46**:1928
- [47] Maeda H, Fukuda T, Kakeshita T. *Journal of Alloys and Compounds*. 2011;**509**:7840
- [48] Porcar L, Bourgault D, Courtois P. *Applied Physics Letters*. 2012;**100**:152405
- [49] Singh S, Nayak J, Rai A, Rajput P, Hill AH, Barman SR, et al. *Journal of Physics: Condensed Materials*. 2013;**25**:212203
- [50] Ahuja BL, Gulzar Ahmed S, Banik M, Itou YS, Barman SR. *Physical Review B*. 2009;**79**:214403

- [51] Singh S, Petricek V, Rajput P, Hill AH, Suard E, Barman SR, et al. *Physical Review B*. 2014;**90**:014109
- [52] Straka L, Heczko O. *Journal of Applied Physics*. 2003;**93**:10
- [53] Banik S, Chakrabarti A, Kumar U, Mukhopadhyay PK, Awasthi AM, Ranjan R, et al. *Physical Review B*. 2006;**74**:085110
- [54] Kamarad J, Albertini F, Arnold Z, Casoli F, Pareti L, Paoluzi A. *Journal of Magnetism and Magnetic Materials*. 2005;**290**:669
- [55] Kira T, Mutata K, Inoue S, Koterazawa K, Jeong SJ, Yang GS, et al. *Materials Transactions*. 2004;**45**:1895
- [56] Kharis Mulyukov Y, Musabirov I. *Journal of Electromagnetic Analysis and Applications*. 2010;**2**:431
- [57] Babita I, Manivel Raja M, Gopalan R, Chandrasekaran V, Ram S. *Journal of Alloys and Compounds*. 2007;**432**:23
- [58] Banik S, Rawat R, Mukhopadhyay PK, Ahuja BL, Chakrabarti A, Paulose PL, et al. *Physical Review B*. 2008;**77**:224417
- [59] Mandal K, Pal D, Scheerbaum N, Lyubina J, Gutfleisch O. *Journal of Applied Physics*. 2009;**105**:073509
- [60] Esakki Muthu S, Rama Rao NV, Manivel Raja M, Arumugam S, Matsubayasi K, Uwatoko Y. *Journal of Applied Physics*. 2011;**110**:083902
- [61] Ma SC, Xuan HC, Zhang CL, Wang LY, Cao QQ, Wang DH, et al. *Applied Physics Letters*. 2010;**97**:052506
- [62] Nayak AK, Suresh KG, Nigam AK, Coelho AA, Gama S. *Journal of Applied Physics*. 2009;**106**:053901
- [63] Roy S, Blackburn E, Valvidares SM, Fitzsimmons MR, Vogel SC, Khan M, et al. *Physical Review B*. 2009;**79**:235127
- [64] Ma Y, Awaji S, Watanabe K, Matsumoto M, Kobayashi N. *Applied Physics Letters*. 2000;**76**(37):65
- [65] Chakrabarti A, Biswas C, Banik S, Dhaka RS, Shukla AK, Barman SR. *Physical Review B*. 2005;**72**:073103
- [66] Elliott RS, Shaw JA, Triantafyllidis N. *International Journal of Solids and Structures*. 2002;**39**:3845
- [67] Fabbri S, Porcari G, Cugini F, Solzi M, Kamarad J, Arnold Z, et al. *Entropy*. 2014;**16**:2204
- [68] Ranjan R, Banik S, Barman SR, Kumar U, Mukhopadhyay PK, Pandey D. *Physical Review B*. 2006;**74**:224443
- [69] Gratz E, Zuckermann HJ. *Journal of Magnetism and Magnetic Materials*. 1982;**29**:181
- [70] Lee Y, Rhee JY, Harmon BN. *Physical Review B*. 2002;**66**:054424
- [71] Burgaro C, Rabe KM, Dal Corso A. *Physical Review B*. 2003;**68**:134104
- [72] <https://journals.aps.org/prb/abstract/10.1103/PhysRevB.79.092410>